A Gold(I) Mononuclear Complex and Its Association into Binuclear and Cluster Compounds by Hydrogen Bonding or Metal Ion Coordination

Leijun Hao,[†] M. Adnan Mansour,[†] Rene J. Lachicotte,[†] Henry J. Gysling,[‡] and Richard Eisenberg*,[†]

Science and Technology Center for Photoinduced Charge Transfer and Department of Chemistry, University of Rochester, Rochester, New York 14627-0216, and Imaging Materials Division, Research and Development Laboratories, Eastman Kodak Company, Rochester, New York 14650-2109

Received April 14, 2000

The mononuclear Au(I) complex, Au(Spy)(PPh_2py) (**1**), has been synthesized and characterized structurally. The complex possesses the expected linear coordination geometry with a S−Au−P bond angle of 176.03(6)° and no evidence of aurophilic interactions between nearest neighbor Au(I) ions in the solid state. Protonation of the pendant pyridyl groups of **1** leads to the formation of the H-bonded dimer [{Au(SpyH)(PPh_2py)}$_2$](PF_6)$_2$ (**2**), which has also been structurally characterized. A linear coordination geometry at the Au(I) ions in **2** with a S−Au−P bond angle of 173.7(2)° is augmented by evidence of a strong aurophilic interaction with a Au···Au distance of 2.979(1) Å. The pendant pyridyl groups of **1** have also been used to bind Cu(I) by reactions with [Cu(NCMe)$_4$](PF_6) and Cu(P(*p*-tolyl)$_3$)$_2$(NO_3) leading to the formation of the heterobimetallic complexes [{AuCu(μ-Spy)(μ-PPh_2py)}$_2$](PF_6)$_2$ (**3**) and [AuCu(P(*p*-tolyl)$_3$)$_2$(μ-Spy)(μ-PPh_2py)](NO_3) (**4**), respectively. A structure determination of **3** reveals a tetranuclear complex composed of two AuCu(μ-Spy)(μ-PPh_2py)$^+$ units held together by bridging thiolate ligands. A strong metal−metal interaction is noted between the two different d^{10} ions with nearest Au−Cu distances averaging 2.6395 Å. The S−Au−P bond angles in **3** deviate slightly from linearity due to the Au···Cu interactions, while the coordination geometries at Cu(I) are distorted tetrahedral consisting of the two pyridyl nitrogen atoms, a bridging thiolate sulfur, and the interacting Au(I) ion. While mononuclear complex **1** is only weakly emissive in the solid state and in fluid solution, complexes **2**−**4** show stronger photoluminescence in the solid state and rigid media at 77 K, and in fluid solution. The emission maxima for **2**−**4** in ambient temperature fluid solution are 470, 635, and 510 nm, respectively. A tentative assignment of the emitting state as a S(pπ) → Au LMCT transition is made on the basis of previous studies of Au(I) thiolate phosphine complexes. Shifts of λ_{em} result from the influence of H bonding or Cu(I) coordination on the filled thiolate orbital energy, or on the effect of metal−metal interaction on the Au(I) acceptor orbital energy. Crystal data for Au(Spy)(PPh_2py) (**1**): triclinic, space group $P\bar{1}$ (No. 2), with $a = 8.3975(4)$ Å, $b = 11.0237(5)$ Å, $c = 12.4105(6)$ Å, $\alpha = 98.6740(10)°$, $\beta = 105.3540(10)°$, $\gamma = 110.9620(10)°$, $V = 995.33(8)$ Å^3, $Z = 2$, R1 = 3.66% ($I > 2\sigma(I)$), wR2 = 9.04% ($I > 2\sigma(I)$) for 2617 unique reflections. Crystal data for [{Au(SpyH)(PPh_2py)}$_2$](PF_6)$_2$ (**2**): triclinic, space group $P\bar{1}$ (No. 2), with $a = 14.0284(3)$ Å, $b = 14.1093(3)$ Å, $c = 15.7027(2)$ Å, $\alpha = 97.1870(10)°$, $\beta = 96.5310(10)°$, $\gamma = 117.1420(10)°$, $V = 2692.21(9)$ Å^3, $Z = 2$, R1 = 7.72% ($I > 2\sigma(I)$), wR2 = 15.34% ($I > 2\sigma(I)$) for 5596 unique reflections. Crystal data for [{AuCu(μ-Spy)(μ-PPh_2py)}$_2$](PF_6)$_2$ (**3**): monoclinic, space group $P2_1/c$ (No. 14), with $a = 19.6388(6)$ Å, $b = 16.3788(4)$ Å, $c = 17.2294(5)$ Å, $\beta = 91.48°$, $V = 5540.2(3)$ Å^3, $Z = 4$, R1 = 3.99% ($I > 2\sigma(I)$), wR2 = 8.38% ($I > 2\sigma(I)$) for 10597 unique reflections.

Introduction

Interest in Au(I) compounds has been stimulated by a number of factors including their real or potential application in diverse areas such as luminescence-based sensors,[1−3] chemical sensitizers of photographic emulsions,[4−9] and antiarthritis drugs.[10−15] The electronic structures of Au(I) compounds have been studied extensively.[16−19] In part because of relativistic effects, these systems exhibit a well-documented tendency to aggregate via

[†] University of Rochester.
[‡] Eastman Kodak Company.

(1) Chan, W.-H.; Mak, T. C. W.; Che, C.-M. *J. Chem. Soc., Dalton Trans.* **1998**, 2275−2276.
(2) Vickery, J. C.; Olmstead, M. M.; Fung, E. Y.; Balch, A. L. *Angew. Chem., Int. Ed. Engl.* **1997**, *36*, 1179−1181.
(3) Mansour, M. A.; Connick, W. B.; Lachicotte, R. J.; Gysling, H. J.; Eisenberg, R. *J. Am. Chem. Soc.* **1997**, *117*, 11329-1330.
(4) Deaton, J. C. Photographic Silver Halide Material Comprising Gold Compound; U.S. Patent 5,049,485; Eastman Kodak Co., 1991.
(5) Deaton, J. C. Photographic Silver Halide Material and Process; U.S. Patent 5,049,484; Eastman Kodak Co., 1991.
(6) Deaton, J. C. Photgraphic Silver Halide Material Comprising Gold Compound; U.S. Patent 5,220,030; Eastman Kodak Co., 1993.
(7) Lok, R.; White, W. W. Photographic Element Containing New Gold-(I) Compounds; U.S. Patent 5,620,841; Eastman Kodak Co., 1997.
(8) Lushington, K. J.; Gysling, H. J. Gold Chemical Sensitizers for Silver Halides; U.S. Patent 5,759,761; Eastman Kodak Co., 1998.
(9) Deaton, J. C.; Luss, H. R. *J. Chem. Soc., Dalton Trans.* **1999**, 3163.
(10) Dash, K. C.; Schmidbaur, H. In *Metal Ions in Biological Systems*; Sigel, H., Ed.; Marcel Dekker: New York, 1982; Vol. 14, p 179.
(11) Sadler, P. J. *Adv. Inorg. Chem.* **1991**, *36*, 1 and references therein.
(12) Lorber, A.; Simon, T. M. *Gold Bull.* **1979**, *12*, 149.
(13) Coffer, M. T.; Shaw, C. F., III; Eidsness, M. K.; Watkins, J. W., II; Elder, R. C. *Inorg. Chem.* **1986**, *25*, 333−339.
(14) Brown, D. H.; Smith, W. E. *Chem. Soc. Rev.* **1980**, *9*, 217.
(15) Parish, R. V.; Cottrill, S. M. *Gold Bull.* **1987**, *20*, 3 and references therein.
(16) Schmidbaur, H. *Gold Bull.* **1990**, *23*, 11.
(17) Schmidbaur, H. *Chem. Soc. Rev.* **1996**, 397.
(18) Pyykkö, P. *Chem. Rev.* **1997**, *97*, 597.

10.1021/ic000396f CCC: $19.00
Published on Web 11/08/2000

aurophilic interactions. The luminescence of Au(I) complexes has been interpreted on the basis of aurophilic interactions in which a degree of metal−metal bonding plays a role.[19,20] The relative importance of aurophilic interactions, hydrogen bonding and π-stacking have been considered with regard to the types of solid-state structures and packing arrangements that Au(I) systems adopt.[21−27]

As part of an effort to develop compounds capable of serving as luminescence-based sensors, the present study reports on the use of supramolecular interactions in the form of H bonding and metal ion coordination to form a binuclear complex and heterobimetallic compounds from a mononuclear Au(I) system. The resultant complexes exhibit luminescence which is stronger than that seen for the d^{10} monomer alone. The occurrence of luminescence from heterobimetallic gold compounds has been described previously, but the reports are relatively few in number.[28−35] They include $[AuIr(CO)Cl(\mu\text{-dppm})_2](PF_6)$ with $d^{10}-d^8$ interactions[30] and $[AuTl(C_6F_5)_2(OPPh_3)_2]_n$ with $d^{10}-s^2$ interactions.[36] Another luminescent Au(I)−Tl(I) system, $AuTl(Ph_2PCH_2S)_2$, is reported to possess a one-dimensional metal−metal bonded polymeric structure in the solid state.[37] Interactions of Au(I) ions with other d^{10} ions such as Ag(I) and Cu(I) have also been described including triangular gold(I) "sandwich" complexes with Ag(I), as well as with Tl(I), that are found to be luminescent.[38] In these latter systems having the general formula $[M[Au_3(\mu\text{-}C^2,N^3\text{-bzim})_3]^+$ (M = Ag, Tl; bzim = 1-benzylimidazolate) as well as in $[Tl[Au_3(\mu\text{-}C(OEt){=}NC_6H_4\text{-}CH_3)_3]^+$, the strong visible luminescence is sensitive to temperature and the metal ion M^+.[38,39]

The present study describes the synthesis, structural characterization, and emission spectroscopy of new gold(I) compounds with thiol and phosphine ligands containing pendant pyridyl groups. Through either protonation and subsequent H bonding or Cu(I) metal ion coordination, the uncoordinated pyridyl groups of the mononuclear complex $Au(Spy)(PPh_2py)$ (**1**) act to form the dicationic binuclear complex $[\{Au(SpyH)(PPh_2py)\}_2](PF_6)_2$ (**2**) or the $[\{AuCu(\mu\text{-Spy})(\mu\text{-}PPh_2py)\}_2](PF_6)_2$ (**3**) and $[AuCu(P(p\text{-tolyl})_3)_2(\mu\text{-Spy})(\mu\text{-}PPh_2py)](NO_3)$ (**4**) heterobimetallic systems, all of which exhibit increased luminescence relative to **1**.

Experimental Section

Chemicals. 2-Pyridinethiol (HSpy) (Aldrich), diphenyl-2-pyridylphosphine (PPh_2py) (Aldrich), and $K[AuCl_4]$ (Strem) were used as received. Reagent grade acetone, acetonitrile, diethyl ether (Et_2O), and 2-propanol (*i*-PrOH) were deoxygenated with an N_2 purge, but otherwise used as received from Aldrich or Fisher Chemical. Spectroscopic grade *N*,*N*-dimethylformamide (DMF), methanol (MeOH), and dichloromethane (CH_2Cl_2) were used as received from Burdick and Jackson. The complexes $Au(SMe_2)Cl$, $[Cu(NCMe)_4](PF_6)$, and $Cu(P(p\text{-tolyl})_3)_2(NO_3)$ were prepared as described in the literature.[40−43]

Physical Measurements. ^1H and $^{31}P\{^1H\}$ NMR spectra were recorded on a Bruker AMX-400 spectrometer operating at 400 and 161.9 MHz, respectively. Chemical shifts are referenced relative to TMS and 85% H_3PO_4; ^1H shifts were determined on the basis of residual proton solvent resonances. Infrared spectra were recorded on a Mattson Galaxy 6020 FTIR spectrophotometer as KBr pellets. Absorption spectra were recorded on a Hitachi U2000 UV−visible spectrophotometer. Steady-state emission measurements were performed on a Spex Fluorolog-2 fluorescence spectrophotometer equipped with a 450 W xenon lamp and Hamamatsu R929 photomultiplier tube detector. Room temperature measurements were made using 1 cm × 1 cm quartz fluorescence cells; solutions were freeze−pump−thaw degassed 4 times and then placed under high-purity nitrogen. Low-temperature emission spectra were recorded in solvent glasses formed in 4 mm diameter quartz EPR tubes placed in a liquid nitrogen dewar equipped with quartz windows. Emission was collected at 90° from the excitation for both experiments. Field desorption mass spectra (FDMS) were measured on a JEOL JMS-HX110 double-focusing mass spectrometer (Kodak Research Laboratories); the reported molecular ion peaks correspond to the most intense peak in a polyisotopic pattern. Elemental analyses were performed by the Analytical Technology Division, Kodak Research Laboratories and Quantitative Technologies Inc.

Au(Spy)(PPh_2py) (1). PPh_2py (319 mg, 1.21 mmol) was added to a solution of $Au(SMe_2)Cl$ (357 mg, 1.21 mmol) in CH_2Cl_2 (30 mL). After 10 min of stirring, a solution of predissolved 2-pyridinethiol (135 mg, 1.21 mmol) and NaOMe (65.5 mg, 1.21 mmol) in MeOH (15 mL) was added dropwise. A white suspension formed immediately. After 1 h of stirring, the solvent was removed by rotary evaporation to give a pale yellow solid, which was extracted with CH_2Cl_2 (2 × 30 mL). After the solution was concentrated to ca. 2 mL, pentane (50 mL) was added to precipitate the product. Filtration followed by washing with diethyl ether afforded a pale yellow powder in 70% yield. X-ray quality crystals were grown by slow diffusion of ether into a CH_2Cl_2 solution of the complex. Anal. Calcd for $C_{22}H_{18}AuN_2PS$: C, 46.33; H, 3.18; N, 4.91; S, 5.62. Found: C, 46.21; H, 3.36; N, 4.78; S, 5.57. ^1H NMR (δ, in CD_2Cl_2): 8.80 (d, ^3J = 4.7 Hz, 1H, H^6-pyP), 8.24 (d, ^3J = 6.0 Hz, 1H, H^6-pyS), 8.07 (t, ^3J = 7.6 Hz, 1H), 7.80 (m, 5H, Ph), 7.50 (m, 6H, py, Ph), 7.41 (m, 2H, py), 7.32 (td, J = 7.9 Hz, J = 1.9 Hz, 1H, py), 6.86 (tm, ^3J = 6.1 Hz, 1H, py). ^{31}P NMR (δ, in CD_2Cl_2): 37.3 (s, 1P). MS-FD (*m*/*z*): 1030 [$(pyPh_2PAu)_2Spy^+$, 100%], 570 [M^+, 27%], 263 [PPh_2py^+, 59%].

[{Au(SpyH)(PPh_2py)}$_2$](PF$_6$)$_2$ (2). Method A. To a solution of Au(Spy)(PPh_2py) (200 mg, 0.351 mmol) in CH_2Cl_2/MeOH (40 mL, 1/1, v/v) was added 1 equiv of HPF_6 (60 wt %) solution (52 μL). After 30 min of stirring, a colorless solution formed. The solvent was then

(19) King, C.; Wang, J.-C.; Khan, M. N. I.; Fackler, J. P., Jr. *Inorg. Chem.* **1989**, *28*, 2145−2149.
(20) Forward, J. M.; Fackler, J. P., Jr.; Assefa, Z. In *Optoelectronic Properties of Inorganic Compounds*; Plenum Press: New York, 1998.
(21) Vicente, J.; Chicote, M.-T.; Abrisqueta, M.-D.; Guerrero, R.; Jones, P. G. *Angew. Chem., Int. Ed. Engl.* **1997**, *36*, 1203−1205.
(22) Onaka, S.; Katsukawa, Y.; Yamashita, M. *Chem. Lett.* **1998**, 525.
(23) Tzeng, B.-C.; Che, C.-M.; Peng, S.-M. *Chem. Commun.* **1997**, 1771−1772.
(24) Puddephatt, R. J. *Chem. Commun.* **1998**, 1055−1062.
(25) Mingos, D. M. P. *J. Chem. Soc., Dalton Trans.* **1996**, 561−566.
(26) Hao, L.; Lachicotte, R. J.; Gysling, H. J.; Eisenberg, R. *Inorg. Chem.* **1999**, *38*, 4616−4617.
(27) Hollatz, C.; Schier, A.; Schmidbaur, H. *J. Am. Chem. Soc.* **1997**, *119*, 8115−8116.
(28) Chan, W.-H.; Cheung, K.-K.; Mak, T. C. W.; Che, C.-M. *J. Chem. Soc., Dalton Trans.* **1998**, 873−874.
(29) Chan, C.-K.; Guo, C.-X.; Cheung, K.-K.; Li, D.; Che, C.-M. *J. Chem. Soc., Dalton Trans.* **1994**, 1677−3682.
(30) Balch, A. L.; Catalano, V. J.; Olmstead, M. M. *Inorg. Chem.* **1990**, *29*, 585−586.
(31) Fernandez, E. J.; Gimeno, M. C.; Jones, P. G.; Laguna, A.; Laguna, M.; Olmos, E. *J. Chem. Soc., Dalton Trans.* **1996**, 3603−3608.
(32) Wang, S.; Garzon, G.; King, C.; Wang, J.-C.; Fackler, J. P., Jr. *Inorg. Chem.* **1989**, *28*, 4623−4629.
(33) Balch, A. L.; Nagle, J. K.; Oram, D. E.; Reedy, J., P. E. *J. Am. Chem. Soc.* **1988**, *110*, 454−462.
(34) Balch, A. L.; Catalano, V. J. *Inorg. Chem.* **1991**, *30*, 1302−1308.
(35) Murray, H. H.; Briggs, D. A.; Garzon, G.; Raptis, R. G.; Porter, L. C.; Fackler, J., J. P. *Organometallics* **1987**, *6*, 1992−1995.
(36) Crespo, O.; Fernandez, E. J.; Jones, P. G.; Laguna, A.; Lopez-de-Luzuriaga, J. M.; Mendia, A.; Monge, M.; Olmos, E. *Chem. Commun.* **1998**, 2233−2234.
(37) Wang, S.; Fackler, J., J. P.; King, C.; Wang, J. C. *J. Am. Chem. Soc.* **1988**, *110*, 3308−3310.
(38) Burini, A.; Fackler, J., J. P.; Galassi, R.; Pietroni, B. R.; Staples, R. J. *Chem. Commun.* **1998**, 95.
(39) Burini, A.; Bravi, R.; Fackler, J., J. P.; Galassi, R.; Grant, T. A.; Omary, M. A.; Pietroni, B. R.; Staples, R. J. *Inorg. Chem.* **2000**, *39*, 3158−3165.
(40) Bonati, F.; Minghetti, G. *Gazz. Chim. Ital.* **1973**, *103*, 373.
(41) Tamaki, A.; Kochi, J. K. *J. Organomet. Chem.* **1974**, *64*, 411−425.
(42) Kubas, G. J. *Inorg. Synth.* **1990**, *28*, 68−70.
(43) Gysling, H. J. *Inorg. Synth.* **1979**, *19*, 92−97.

removed under vacuum. The white residue was extracted with CH_2Cl_2 (2 × 30 mL). Concentration of this solution to ca. 2 mL followed by addition of diethyl ether gave the product as a white solid. Yield: 92%. X-ray quality crystals were grown by slow diffusion of ether into a CH_2Cl_2 solution of the complex. Anal. Calcd for $C_{44}H_{36}F_{12}Au_2N_4P_4S_2$: C, 36.94; H, 2.54; N, 3.92. Found: C, 37.37; H, 2.71; N, 3.64. IR (KBr): ν(N−H) = 3288 cm^{-1} (br, w), δ (NH) = 1984 (br, w) cm^{-1}. ^{1}H NMR (δ in CD_2Cl_2): 13.0 (br, 1H, H−N), 8.86 (d, 1H, J = 4.4 Hz, H^6-pyP), 8.15 (d, 1H, J = 5.9 Hz, H^6-pyS), 7.87 (m, 3H, py), 7.6−7.4 (m, 12H), 7.30 (tm, 1H, J = 6.7, py). ^{31}P NMR (δ, in CD_2Cl_2): 37.8 (s) with a resonance for PF_6^- also present −92.6 ppm.

Method B. To a solution of Au(PPh$_2$py)Cl[44] (201 mg, 0.406 mmol) in dry THF (30 mL) was added $AgPF_6$ (103 mg, 0.406 mmol). After 5 min of stirring, a white precipitate formed. Pyridine-2-thiol was then added to this solution. After 10 min of stirring, the pale yellow suspension was evaporated to dryness. The solid was extracted with CH_2Cl_2 (2 × 30 mL). The extract was concentrated to ca. 2 mL, and diethyl ether was added to precipitate the product as a white solid. Yield: 91%. This product was characterized by ^{1}H and ^{31}P NMR spectroscopies, which gave spectra identical to those of a sample obtained by method A.

[{AuCu(μ-Spy)(μ-PPh$_2$py)}$_2$](PF$_6$)$_2$ (3). To a solution of **1** (442 mg, 0.775 mmol) in CH_2Cl_2 (50 mL) was added [Cu(NCMe)$_4$][PF$_6$] (289 mg, 0.775 mmol). A yellow suspension formed immediately. The mixture was allowed to stir overnight under subdued light. The yellow solution was then filtered and concentrated to ca. 2 mL. Diethyl ether was added to precipitate the product followed by filtration, washing with diethyl ether and hexane to afford an orange-yellow crystalline solid in 90% yield. Anal. Calcd for $C_{22}H_{18}F_6N_2P_2SAuCu$: C, 33.92; H, 2.33; N, 3.60. Found: C, 33.20; H, 2.35; N, 3.41. ^{1}H NMR (δ in CD_2Cl_2): 9.26 (s, br, 1H, H^6-pyP), 8.20 (s, br, 1H, H^6-pyS), 7.99 (s, br, 1H, pyS), 7.82 (s, br, 1H, pyS), 7.6−7.4 (m, 13H), 7.04 (s, br, 1H, py). ^{31}P NMR (δ in CD_2Cl_2): 39.1 (s, 1P) with a resonance for PF_6^- also present.

[AuCu(P(p-tolyl)$_3$)$_2$(μ-Spy)(μ-PPh$_2$py)](NO$_3$) (4). The light yellow compound **4** was prepared by a procedure similar to that used for **3** but with Cu(P(*p*-tolyl)$_3$)$_2$(NO$_3$) instead of [Cu(NCMe)$_4$](PF$_6$). Yield: 79%. Anal. Calcd for $C_{50}H_{42}N_3P_3SAuCu$: C, 58.92; H, 4.64; N, 3.22. Found: C, 61.25; H, 4.94; N, 2.51. ^{1}H NMR (δ in CD_2Cl_2): 8.48 (d, br, 1H, py), 7.56 (tm, br, 1H, J = 7.6 Hz, py), 7.41 (m, br, 2H, py), 7.3−7.1 (m, 38H), 2.37 (s, 18H, CH_3). ^{31}P NMR (δ in CD_2Cl_2): 39.7 (s, br, 2P), 27.1 (s, br, 1P).

X-ray Structural Determination of 1. A colorless crystal of approximate dimensions 0.22 × 0.18 × 0.08 mm^3 was mounted under Paratone-8277 onto a glass fiber and immediately placed in a cold nitrogen stream at −80 °C on the X-ray diffractometer. The X-ray intensity data were collected on a standard Siemens SMART CCD area detector system equipped with a normal focus molybdenum-target X-ray tube operated at 2.0 kW (50 kV, 40 mA). A total of 1321 frames of data (1.3 hemispheres) were collected using a narrow-frame method with scan widths of 0.3° in ω and exposure times of 10 s/frame using a detector-to-crystal distance of 5.09 cm (maximum 2θ angle of 56.5°). The total data collection time was approximately 6 h. Frames were integrated to a maximum 2θ angle of 46.5° with the Siemens SAINT program to yield a total of 4460 reflections, of which 2808 were independent (R_{int} = 5.27%, R_{sig} = 5.04%) and 2617 were above 2σ(I). Laue symmetry revealed a triclinic crystal system, and the final unit cell parameters (at −80 °C) were determined from the least-squares refinement of three-dimensional centroids of 3868 reflections.

The space group was assigned as $P\bar{1}$ (No. 2), and the structure was solved by using direct methods and refined employing full-matrix least-squares on F^2 (Siemens, SHELXTL, version 5.04). For a Z value of 2, there is one independent molecule in the asymmetric unit. All of the atoms were refined with anisotropic thermal parameters, and hydrogen atoms were included in idealized positions, giving a data:parameter ratio of greater than 10:1. The structure refined to a goodness of fit (GOF) of 1.038 and final residuals of R1 = 3.66% ($I > 2\sigma(I)$), wR2 = 9.04% ($I > 2\sigma(I)$).

(44) Schmidbaur, H.; Inoguchi, Y. *Z. Naturforsch.* **1980**, 1329.

X-ray Structural Determination of 2. Crystals were grown from CH_2Cl_2/Bz/Et_2O under ambient conditions in an NMR tube. A colorless crystal of approximate dimensions 0.08 × 0.04 × 0.02 mm^3 was mounted under Paratone-8277 on a glass fiber and immediately placed in a cold nitrogen stream at −80 °C on the X-ray diffractometer. The X-ray intensity data were collected as for **1** with exposure times of 60 s/frame and total data collection time of 27 h. Frames were integrated to a maximum 2θ angle of 46.6° to yield a total of 11367 reflections, of which 7246 were independent (R_{int} = 3.64%, R_{sig} = 8.28%) and 5596 were above 2σ(I). Laue symmetry revealed a triclinic crystal system, and the final unit cell parameters (at −80 °C) were determined from the least-squares refinement of three-dimensional centroids of 5512 reflections.

The space group was assigned as $P\bar{1}$ (No. 2), and the structure was solved as for **1**. For a Z value of 2, one Au dimer and two PF_6 counterions as well as one CH_2Cl_2 solvent molecule and two H_2O molecules were located in the asymmetric unit. All of the non-H atoms of the cation and anions except C36, which had a tendency toward nonpositive definite thermal parameters, were refined anisotropically, and the hydrogen atoms were included in idealized positions. The solvent molecules were refined with isotropic thermal parameters. H atoms for one of the water molecules (O1) were located, and positions and isotropic thermal parameters were fixed. The CH_2Cl_2 molecule and one of the water molecules (O2) were refined at half-occupancy, due to high isotropic thermal parameters at full occupancy. This assumption seems reasonable due to the fact that these crystals appear to lose solvent rapidly upon removal from the crystallization solvents. It should also be noted that although the source of H_2O is unknown, the assignment as water is reasonable since both exhibit a strong H-bonding pattern typical of water. Unfortunately, there are two large peaks (ca. 2 e$^-$/Å^3, 1.7 Å from C22 and 1.4 Å from S2) for which no suitable model could be found. The final data$_{obs}$:parameter ratio was 9:1. The structure refined to a GOF of 1.165 and final residuals of R1 = 7.72% ($I > 2\sigma(I)$), wR2 = 15.34% ($I > 2\sigma(I)$).

X-ray Structural Determination of 3. A pale metallic green crystal of approximate dimensions 0.16 × 0.13 × 0.16 mm^3 was mounted under Paratone-8277 on a glass fiber and immediately placed in a cold nitrogen stream at −80 °C on the X-ray diffractometer. The X-ray intensity data were collected as for **1** with exposure times of 30 s/frame and total data collection time of 13 h. Frames were integrated to a maximum 2θ angle of 56.6° with the Siemens SAINT program to yield a total of 32083 reflections, of which 12783 were independent (R_{int} = 2.87%, R_{sig} = 4.06%) and 10597 were above 2σ(I). Laue symmetry revealed a monoclinic crystal system, and the final unit cell parameters (at −80 °C) were determined from the least-squares refinement of three-dimensional centroids of 8192 reflections.

The space group was assigned as $P2_1/c$, and the structure was solved as for **1**. For a Z value of 4, one molecule and one $C_6H_4Cl_2$ were located in the asymmetric unit. All of the non-H atoms of the cation and solvent molecule were refined anisotropically, and the hydrogen atoms were included in idealized positions. The fluorine atoms of both PF_6 counterions were found to be disordered over two positions, and the disordered atoms were refined isotropically. The final data$_{obs}$:parameter ratio was >18:1. The structure refined to a GOF of 1.037 and final residuals of R1 = 3.99% ($I > 2\sigma(I)$), wR2 = 5.39% ($I > 2\sigma(I)$).

Results and Discussion

Synthesis and Structural Characterization of the Mononuclear Complex Au(Spy)(PPh$_2$py) (1). 1 was conveniently prepared by reaction of Au(Me$_2$S)Cl with PPh$_2$py and Na(2-Spy), generated in situ from equimolar amounts of 2-HSpy and NaOMe in methanol solution. The spectroscopic characterization of **1** is consistent with a Au(I) product having a 1:1 ratio of PPh$_2$py and Spy$^-$ ligands. Specifically, the ^{31}P NMR spectrum of **1** in CD_2Cl_2 contains a single resonance at δ 37.3 ppm due to the phosphorus atom of the PPh$_2$py ligand, while the ^{1}H NMR spectrum shows two doublet resonances for the protons ortho to the pyridine N atoms at δ 8.80 and 8.24 ppm for PPh$_2$py and Spy$^-$, respectively.

Table 1. Crystallographic Data for **1**−**3**

crystal params	**1**	**2**	**3**
chem formula	$C_{22}H_{18}AuN_2PS$	$C_{45}H_{42}Au_2Cl_2F_{12}N_4O_2P_4S_2$	$C_{50}H_{40}Au_2Cl_2Cu_2F_{12}N_4P_4S_2$
fw	570.38	1551.66	1704.77
cryst syst	triclinic	triclinic	monoclinic
space group (No.)	$P\bar{1}$ (2)	$P\bar{1}$ (2)	$P2_1/c$ (14)
Z	2	2	4
a, Å[a]	8.3975(4)	14.0284(3)	19.6388(6)
b, Å	11.0237(5)	14.1093(3)	16.3788(4)
c, Å	12.4105(6)	15.7027(2)	17.2294(5)
α, deg	98.6740(10)	97.1870(10)	90.00
β, deg	105.3540(10)	96.5310(10)	91.48
γ, deg	110.9620(10)	117.1420(10)	90.00
vol, Å^3	995.33(8)	2692.21(9)	5540.2(3)
ρ_{calcd}, g cm^{-3}	1.903	1.914	2.044
cryst dimens, mm^3	0.08 × 0.18 × 0.22	0.02 × 0.04 × 0.08	0.13 × 0.13 × 0.16
temp, K	193(2)	193(2)	193(2)
radiation	Mo, 0.71073 Å	Mo, 0.71073 Å	Mo, 0.71073 Å
no. of obsd data ($I > 2\sigma(I)$)	2617	5596	10597
no. of params varied	244	628	691
μ, cm^{-1} [b]	7.584	5.822	6.405
R1(F_o), wR2(F_o^2) ($I > 2\sigma$)[c,d]	0.0366, 0.0904	0.0772, 0.1534	0.0399, 0.0838
R1(F_o), wR2(F_o^2) (all data)	0.0389, 0.0917	0.1020, 0.1633	0.0539, 0.0897

[a] It has been noted that the integration program SAINT produces cell constant errors that are unreasonably small, since systematic error is not included. More reasonable errors might be estimated at 10× the listed value. [b] Data were corrected for absorption with the SADABS program based on the method of Blessing; see: Blessing, R. H. *Acta Crystallogr., Sect. A* **1995**, *51*, 33. [c] *SHELXTL: Structure Analysis Program, version 5.04*; Siemens Industrial Automation Inc.: Madison, WI, 1995. [d] $R1 = (\sum||F_o| - |F_c||)/\sum|F_o|$; $wR2 = [\sum w(F_o^2 - F_c^2)^2]/\sum w(F_o^2)^2]]^{1/2}$ where $w = 1/[\sigma^2(F_o^2) + (aP)^2 + bP]$ and $P = [(\text{Max}; 0, F_o^2) + 2F_c^2]/3$.

Table 2. Atomic Coordinates (×10^4) and Equivalent Isotropic Parameters (Å × 10^3) for **1**

	x	y	z	U(eq)[a]
Au(1)	−18807(1)	−16143(1)	−3242(1)	25(1)
S(1)	−20859(3)	−18291(2)	−3435(2)	32(1)
P(1)	−16959(2)	−13998(2)	−3058(2)	22(1)
N(1)	−14775(9)	−12516(7)	−4075(6)	39(2)
N(2)	−21193(8)	−16729(6)	−1699(6)	34(2)
C(1)	−16151(9)	−13711(6)	−4262(6)	22(2)
C(2)	−14220(11)	−12276(8)	−4989(7)	38(2)
C(3)	−15001(10)	−13196(8)	−6071(7)	32(2)
C(4)	−16418(11)	−14402(8)	−6243(7)	35(2)
C(5)	−17011(9)	−14668(7)	−5328(6)	29(2)
C(6)	−14961(9)	−13216(7)	−1729(6)	24(2)
C(7)	−14365(10)	−14015(8)	−1121(6)	28(2)
C(8)	−12904(10)	−13402(8)	−73(7)	35(2)
C(9)	−12065(10)	−12014(8)	346(7)	35(2)
C(10)	−12663(11)	−11233(9)	−280(7)	41(2)
C(11)	−14108(9)	−11839(7)	−1316(6)	26(2)
C(12)	−18154(9)	−12919(7)	−2943(6)	22(1)
C(13)	−18241(10)	−12038(8)	−3612(7)	31(2)
C(14)	−19211(11)	−11268(8)	−3474(8)	38(2)
C(15)	−20068(11)	−11380(8)	−2669(8)	40(2)
C(16)	−19984(11)	−12255(9)	−1998(8)	43(2)
C(17)	−19037(10)	−13041(7)	−2135(6)	28(2)
C(18)	−21944(10)	−17950(7)	−2462(6)	28(2)
C(19)	−22051(11)	−16506(8)	−984(8)	40(2)
C(20)	−23659(12)	−17457(9)	−981(8)	44(2)
C(21)	−24442(12)	−18708(8)	−1760(8)	44(2)
C(22)	−23558(11)	−18952(7)	−2508(7)	36(2)

[a] U(eq) is defined as one-third of the trace of the orthogonalized $\mathbf{U}_{ij}$ tensor.

The assignment for **1** as a 1:1 complex of PPh_2py and Spy^- with Au(I) is confirmed by a single-crystal X-ray structure determination. In Table 1, crystallographic and data collection parameters for all of the structure determinations are presented. Table 2 contains the final positional and equivalent isotropic thermal parameters for **1** while Table 3 presents selected bond distances and angles for the structure. A complete tabulation of bond distances and angles is given in the Supporting Information. An ORTEP representation of **1** is shown in Figure 1. The crystal structure consists of discrete Au(Spy)(PPh_2py) complexes with no intermolecular aurophilic interactions, the closest Au···Au distance of 5.630(2) Å being well beyond the range for such interactions.[17,20,45,46] The coordination geometry

Table 3. Selected Bond Distances (Å) and Angles (deg) for **1**

Au(1)−P(1)	2.253(2)	C(1)−C(5)	1.383(10)
Au(1)−S(1)	2.308(2)	C(2)−C(3)	1.381(11)
S(1)−C(18)	1.767(7)	C(3)−C(4)	1.370(11)
P(1)−C(6)	1.830(7)	C(4)−C(5)	1.385(11)
N(1)−C(1)	1.342(9)	C(18)−C(22)	1.389(10)
N(1)−C(2)	1.362(11)	C(19)−C(20)	1.384(12)
N(2)−C(19)	1.330(11)	C(20)−C(21)	1.372(12)
N(2)−C(18)	1.340(10)	C(21)−C(22)	1.385(12)

P(1)−Au(1)−S(1)	176.03(6)	N(1)−C(1)−C(5)	122.8(7)
C(18)−S(1)−Au(1)	101.1(2)	N(1)−C(1)−P(1)	116.9(5)
C(1)−P(1)−Au(1)	116.1(2)	C(5)−C(1)−P(1)	120.2(5)
C(12)−P(1)−Au(1)	109.7(2)	N(2)−C(18)−C(22)	121.6(7)
C(6)−P(1)−Au(1)	114.7(2)	N(2)−C(18)−S(1)	119.2(5)
C(1)−N(1)−C(2)	117.0(6)	C(22)−C(18)−S(1)	119.2(6)
C(19)−N(2)−C(18)	117.6(6)		

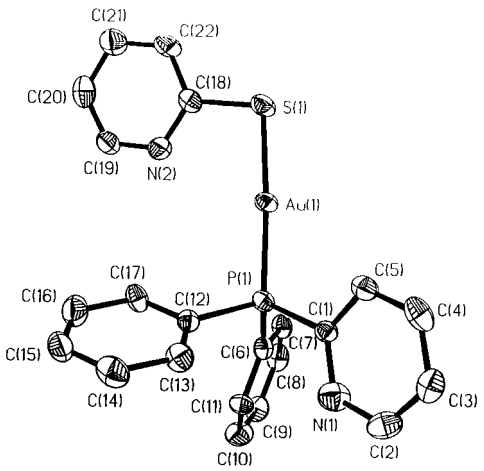

Figure 1. A perspective view of **1**.

(45) Pyykko, P.; Runeberg, N.; Mendizabal, F. *Chem.—Eur. J.* **1997**, *3*, 1451−1457.

Table 4. Atomic Coordinates ($\times 10^4$) and Equivalent Isotropic Parameters (Å $\times 10^3$) for **2**

	x	*y*	*z*	*U*(eq)[a]		*x*	*y*	*z*	*U*(eq)[a]
Au(1)	−651(1)	−5100(1)	−3496(1)	42(1)	C(28)	−2210(13)	−5946(13)	−860(9)	30(4)
Au(2)	127(1)	−4322(1)	−1569(1)	43(1)	C(29)	−1774(15)	−6632(14)	−853(11)	43(5)
S(1)	−841(4)	−6725(4)	−3164(4)	67(2)	C(30)	−2388(20)	−7656(14)	−653(12)	61(7)
S(2)	1753(4)	−4117(5)	−1962(4)	70(2)	C(31)	−3435(19)	−8006(16)	−520(14)	63(6)
P(1)	−424(3)	−3572(3)	−3972(3)	34(1)	C(32)	−3906(17)	−7339(16)	−559(15)	64(6)
P(2)	−1407(4)	−4588(3)	−1056(3)	36(1)	C(33)	−3295(16)	−6304(15)	−768(12)	49(5)
N(1)	−2908(12)	−7187(11)	−3054(10)	45(4)	C(34)	−1081(14)	−3648(13)	−31(11)	38(4)
N(2)	2196(13)	−2048(13)	−1987(10)	51(4)	C(35)	−1546(19)	−3984(17)	649(12)	86(9)
N(3)	112(12)	−2174(11)	−2457(9)	45(4)	C(36)	−1242(21)	−3237(22)	1424(18)	91(8)
N(4)	−2814(11)	−5104(11)	−2567(9)	42(4)	C(37)	−530(22)	−2148(19)	1504(15)	80(8)
C(1)	−2190(17)	−7569(15)	−3160(13)	54(5)	C(38)	−14(19)	−1838(17)	859(17)	79(8)
C(2)	−3971(17)	−7831(17)	−3081(12)	60(6)	C(39)	−252(16)	−2585(15)	75(13)	55(5)
C(3)	−4356(20)	−8900(20)	−3168(17)	79(7)	C(40)	−2369(13)	−4360(12)	−1785(10)	32(4)
C(4)	−3713(25)	−9339(17)	−3241(15)	83(9)	C(41)	−2687(14)	−3618(13)	−1536(12)	41(4)
C(5)	−2627(23)	−8695(16)	−3208(14)	72(7)	C(42)	−3452(16)	−3533(16)	−2138(13)	59(6)
C(6)	2603(16)	−2747(17)	−1918(13)	59(6)	C(43)	−3885(14)	−4243(15)	−2950(12)	47(5)
C(7)	3743(16)	−2338(22)	−1810(15)	74(7)	C(44)	−3544(14)	−5002(15)	−3131(12)	51(5)
C(8)	4410(20)	−1246(25)	−1788(16)	91(9)	P(3)	2868(4)	847(4)	166(4)	54(1)
C(9)	3977(19)	−537(22)	−1839(12)	71(7)	F(1)	1889(13)	1097(14)	252(10)	112(5)
C(10)	2885(17)	−983(16)	−1933(13)	59(6)	F(2)	2896(10)	630(12)	1144(8)	90(4)
C(11)	957(14)	−2714(14)	−4137(10)	38(4)	F(3)	3736(14)	2095(11)	532(11)	134(7)
C(12)	1649(15)	−3154(15)	−4202(13)	50(5)	F(4)	2817(13)	1044(11)	−798(9)	96(5)
C(13)	2690(16)	−2541(18)	−4361(13)	58(6)	F(5)	3857(10)	607(11)	87(9)	92(5)
C(14)	3006(15)	−1493(19)	−4457(13)	60(6)	F(6)	2058(9)	−407(9)	−185(8)	75(4)
C(15)	2317(17)	−1052(17)	−4390(14)	62(6)	P(4)	4168(4)	2127(4)	4811(4)	54(1)
C(16)	1268(17)	−1654(15)	−4232(13)	55(5)	F(7)	2927(10)	1250(12)	4416(11)	118(6)
C(17)	−1363(14)	−3883(14)	−4988(11)	42(4)	F(8)	3925(13)	3081(13)	4727(10)	109(5)
C(18)	−2363(15)	−4772(17)	−5114(15)	64(6)	F(9)	4420(12)	2114(10)	3858(7)	89(4)
C(19)	−3155(17)	−5030(17)	−5843(15)	64(6)	F(10)	5418(10)	2966(10)	5187(8)	82(4)
C(20)	−2933(19)	−4413(21)	−6452(16)	83(8)	F(11)	3936(12)	2135(13)	5763(9)	98(4)
C(21)	−1954(23)	−3497(26)	−6287(19)	149(17)	F(12)	4437(11)	1159(10)	4905(9)	88(4)
C(22)	−1126(18)	−3271(22)	−5611(14)	97(10)	C(1S)	−3923(43)	−3596(40)	1120(34)	89(16)
C(23)	−635(12)	−2618(13)	−3225(11)	37(4)	Cl(1)	−3829(14)	−2827(14)	2139(12)	120(5)
C(24)	24(15)	−1436(14)	−1905(11)	45(5)	Cl(2)	−4354(13)	−4840(13)	1035(11)	111(5)
C(25)	−758(16)	−1110(15)	−2066(14)	54(5)	O(1)	−139(18)	−510(17)	4067(14)	131(7)
C(26)	−1485(18)	−1572(15)	−2807(14)	58(6)	O(2)	−2134(28)	−1167(28)	2842(23)	98(11)
C(27)	−1433(16)	−2334(15)	−3403(12)	52(5)					

[a] *U*(eq) is defined as one-third of the trace of the orthogonalized $\mathbf{U}_{ij}$ tensor.

at the Au(I) center is, as expected, essentially linear with a P−Au−S bond angle of 176.0(1)°. The bond lengths of S(1)−Au(1) and P(1)−Au(1) are 2.308(2) and 2.253(2) Å, respectively, which compare well with previously reported values in Au(I) phosphine thiolate complexes.[47−49]

In view of the noted tendency of Au(I) thiolate complexes to exhibit aurophilic interactions,[48,50] and the fact that Au(SPh)(PPh$_3$) is dimeric,[51] the absence of aurophilic interactions in the structure of **1** was unexpected. However, this absence may be explained by a weak interaction between the Au(I) ion and the pendant pyridyl N atom 3.10 Å away. While clearly not a bond, this weak but significant Au(I)−pyridyl N interaction is suggested by several structural parameters involving the pyridyl-containing ligand. For example, the C−S−Au angle in **1** is 101.1° compared with the analogous parameters of 109.1° and 108.5° in **2** (vide infra). Also, the dihedral angle of Au−S−C−N of 14.0° deviates only slightly from planarity, consistent with an Au···pyridyl N interaction. However, it should be noted that in the structure of **2** discussed below in which there is no Au···pyridyl N interaction, the dihedral angles defined by Au−S−C−N are only 21.3° and 23.1°.

Scheme 1

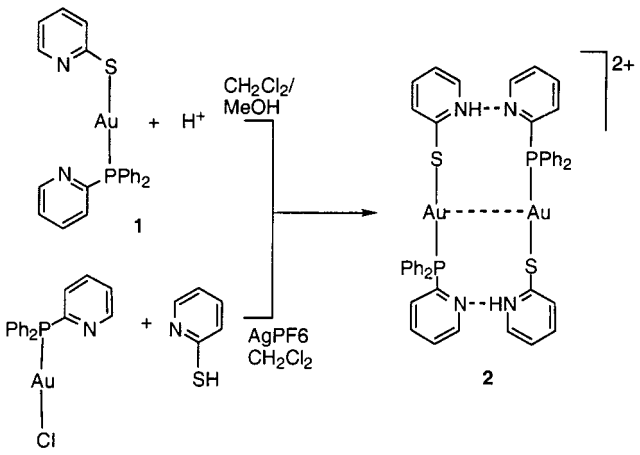

Formation and Characterization of the H-Bonded Binuclear Complex [{Au(SpyH)(PPh$_2$py)}$_2$](PF$_6$)$_2$ (2). Protonation of **1** with acids such as HPF$_6$ results in the formation of the binuclear complex **2** in which monomeric units of Au(SpyH)(PPh$_2$py)$^+$ are held together by two NH···N hydrogen bonds (Scheme 1). Complex **2** can also be prepared in high yield by the reaction of [Au(PPh$_2$py)][PF$_6$], generated from

(46) Pyykko, P.; Mendizabal, F. *Chem.—Eur. J.* **1997**, *3*, 1458−1465.
(47) Narayanaswamy, R.; Young, M. A.; Parkhurst, E.; Ouellette, M.; Kerr, M. E.; Ho, D. M.; Elder, R. C.; Bruce, A. E.; Bruce, M. R. M. *Inorg. Chem.* **1993**, *32*, 2506−2517.
(48) Forward, J. M.; Boohmann, D.; Fackler, J. P.; Staples, R. J. *Inorg. Chem.* **1995**, *34*, 6330−6336.
(49) Tzeng, B.-C.; Chan, C.-K.; Cheung, K.-K.; Che, C.-M.; Peng, S.-M. *Chem. Commun.* **1997**, 135−136.
(50) van Zyl, W. E.; Staples, R. J.; Fackler, J. P. *Inorg. Chem. Commun.* **1998**, *1*, 51.
(51) Nakamoto, M.; Hiller, W.; Schmidbaur, H. *Chem. Ber.* **1993**, *126*, 605−610.

Table 5. Selected Bond Distances (Å) and Angles (deg) for **2**

Au(1)−P(1)	2.267(5)	P(2)−C(34)	1.82(2)
Au(1)−S(1)	2.318(5)	P(2)−C(40)	1.84(2)
Au(1)−Au(2)	2.9785(10)	N(1)−C(2)	1.34(2)
Au(2)−P(2)	2.271(5)	N(1)−C(1)	1.36(2)
Au(2)−S(2)	2.329(5)	N(2)−C(10)	1.35(2)
S(1)−C(1)	1.72(2)	N(2)−C(6)	1.36(2)
S(2)−C(6)	1.73(2)	N(3)−C(24)	1.33(2)
P(1)−C(17)	1.81(2)	N(3)−C(23)	1.37(2)
P(1)−C(23)	1.82(2)	N(4)−C(44)	1.35(2)
P(1)−C(11)	1.83(2)	N(4)−C(40)	1.38(2)
P(2)−C(28)	1.81(2)		

P(1)−Au(1)−S(1)	173.3(2)	C(10)−N(2)−C(6)	120(2)
P(1)−Au(1)−Au(2)	102.93(11)	C(24)−N(3)−C(23)	116(2)
S(1)−Au(1)−Au(2)	82.8(2)	C(44)−N(4)−C(40)	116.4(14)
P(2)−Au(2)−S(2)	173.7(2)	N(1)−C(1)−C(5)	114(2)
P(2)−Au(2)−Au(1)	103.82(11)	N(1)−C(1)−S(1)	122.3(14)
S(2)−Au(2)−Au(1)	81.1(2)	C(5)−C(1)−S(1)	123(2)
C(1)−S(1)−Au(1)	109.1(7)	N(2)−C(6)−C(7)	119(2)
C(6)−S(2)−Au(2)	108.5(8)	N(2)−C(6)−S(2)	121(2)
C(17)−P(1)−C(23)	105.2(8)	C(7)−C(6)−S(2)	120(2)
C(17)−P(1)−C(11)	107.8(8)	C(12)−C(11)−P(1)	118.9(14)
C(23)−P(1)−C(11)	101.7(8)	C(16)−C(11)−P(1)	119.5(14)
C(17)−P(1)−Au(1)	111.7(6)	C(22)−C(17)−P(1)	123.6(14)
C(23)−P(1)−Au(1)	115.4(6)	C(27)−C(23)−P(1)	124.7(13)
C(11)−P(1)−Au(1)	114.1(6)	N(3)−C(23)−P(1)	113.5(12)
C(28)−P(2)−C(34)	106.8(7)	N(3)−C(24)−C(25)	124(2)
C(28)−P(2)−C(40)	104.7(7)	C(29)−C(28)−P(2)	119.7(14)
C(34)−P(2)−C(40)	104.8(7)	C(33)−C(28)−P(2)	119.9(13)
C(28)−P(2)−Au(2)	114.4(6)	C(35)−C(34)−P(2)	121.4(14)
C(34)−P(2)−Au(2)	111.2(6)	C(39)−C(34)−P(2)	118.9(14)
C(40)−P(2)−Au(2)	114.1(6)	N(4)−C(40)−P(2)	112.9(12)
C(2)−N(1)−C(1)	123(2)		

$AuCl(PPh_2py)$ and $AgPF_6$ in THF solution, with the neutral ligand SpyH.

The ^{31}P NMR spectrum of **2** in CD_2Cl_2 shows a singlet resonance at δ 37.8 ppm for PPh_2py and the PF_6^- resonance at δ −92.6 ppm in an integration ratio of 1:1. As for **1**, the ^1H NMR spectrum of **2** displays two doublet resonances for the 6-position protons of the pyridine rings of PPh_2py and Spy ligands at δ 8.86 and 8.15 ppm, respectively. A very broad resonance is also observed at δ 13.0 ppm and is assigned to the protons involved in the hydrogen bonding. The IR spectrum of **2** contains two weak bands at 3288 [ν(NH)] and 1984 [δ(NH)] cm^{-1} which can be compared to those found in the H-bonded systems $[NEt_4]_2[\{Ni(Hbim)]$ (ν(NH) = 2811 cm^{-1}, δ(NH) = 1912 cm^{-1}, Hbim = monoprotonated 2,2′-biimidazole) and $[Ir\{H(\eta^1\text{-}SC_5H_4NH)\}_2(PCy_3)_2][BF_4]$ (ν(NH) = 3184 cm^{-1}).[52,53]

The dimeric nature of **2** was established by a crystal structure analysis. Crystallographic and data collection parameters are summarized in Table 1 while atomic positional and equivalent isotropic thermal parameters are given in Table 4. Selected bond distances and angles are presented in Table 5, and a perspective view of the H-bonded dimer is shown in Figure 2. The coordination geometry at the Au atom deviates slightly from linearity with S(1)−Au(1)−P(1) and S(2)−Au(2)−P(2) bond angles of 173.3(2)° and 173.7(2)°, respectively. The Au−S and Au−P distances are in agreement with those found for **1** and related structures.[47−49] While the protons involved in the H bonding were not located, the separation between the H-bonded N atoms [N(1) and N(4), and N(2) and N(3)] averaged 2.86 Å. Dimer **2**, in addition to being held together by H bonding, shows evidence of strong aurophilic interaction with a Au(1)···Au(2) distance of 2.987(1) Å that is comparable to other dinuclear Au(I) compounds exhibiting such interactions.[3,19,26,47,49]

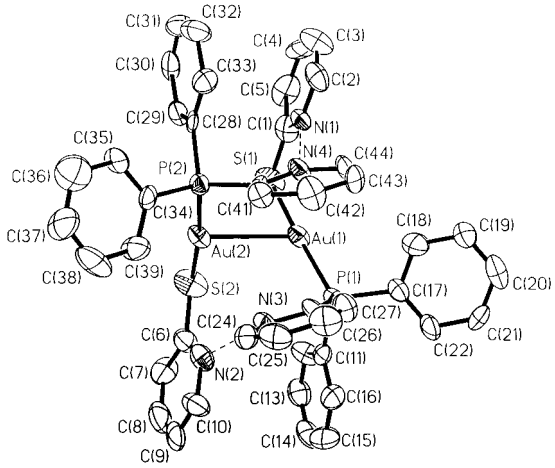

Figure 2. A perspective view of **2**.

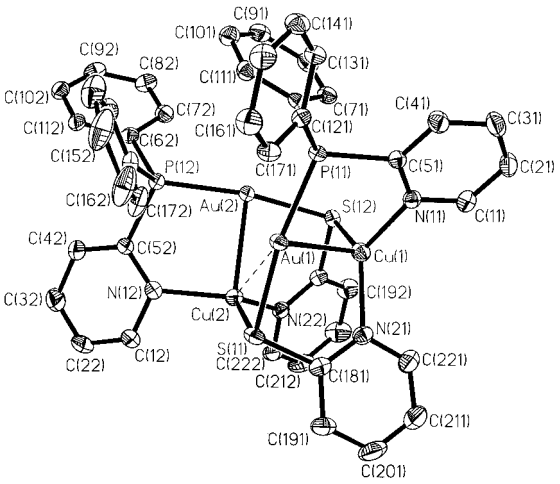

Figure 3. A perspective view of **3**.

Synthesis and Structural Characterization of the $[\{AuCu(\mu\text{-Spy})(\mu\text{-}PPh_2py)\}_2](PF_6)_2$ (3) and $[AuCu(P(p\text{-tolyl})_3)_2(\mu\text{-Spy})(\mu\text{-}PPh_2py)](NO_3)$ (4) Heterobimetallic Systems. As shown in Scheme 2, the reaction of **1** with an equimolar amount of $[Cu(NCMe)_4][PF_6]$ in CH_2Cl_2 solution affords the yellow tetranuclear compound **3** in moderate yield, while the reaction of **1** with $[\{(p\text{-tolyl})_3P\}_2CuNO_3]$ gives the pale yellow heterobinuclear compound **4**. The ^{31}P NMR spectrum of **3** in CD_2Cl_2 contains a single uncoupled resonance at δ 39.1 ppm due to the phosphorus atom of the diphenylpyridylphosphine ligand as well as the resonance for PF_6^-. The ^1H NMR spectrum of **3** displays two resonances for the protons ortho to the N atoms of the PPh_2py and SpyH pyridine rings at δ 9.26 and 8.20 ppm, respectively. The ^{31}P NMR spectrum of **4** in CD_2Cl_2 contains two resonances at δ 39.7 and 27.1 ppm in an integration ratio of 1:2, corresponding to the phosphorus atoms of the diphenylpyridylphosphine and the two tri(*p*-tolyl)phosphine ligands.

The tetranuclear Au_2Cu_2 nature of **3** was confirmed by a single-crystal X-ray structure analysis. A perspective view of the complex is provided in Figure 3 while final positional and equivalent isotropic thermal parameters are given in Table 6 and selected bond distances and angles are presented in Table 7. The crystal structure of **3** reveals the packing of discrete Au_2Cu_2 cluster complexes along with CH_2Cl_2 and H_2O molecules of crystallization. The formation of **3** can be viewed as a

(52) Tadokoro, M.; Isobe, K.; Uekusa, H.; Ohashi, Y.; Toyoda, J.; Tashiro, K.; Nakasuji, K. *Angew. Chem., Int. Ed.* **1999**, *38*, 95−98.
(53) Lough, A. J.; Park, S.; Ramachandran, R.; Morris, R. H. *J. Am. Chem. Soc.* **1994**, *116*, 8356−8357.

Scheme 2

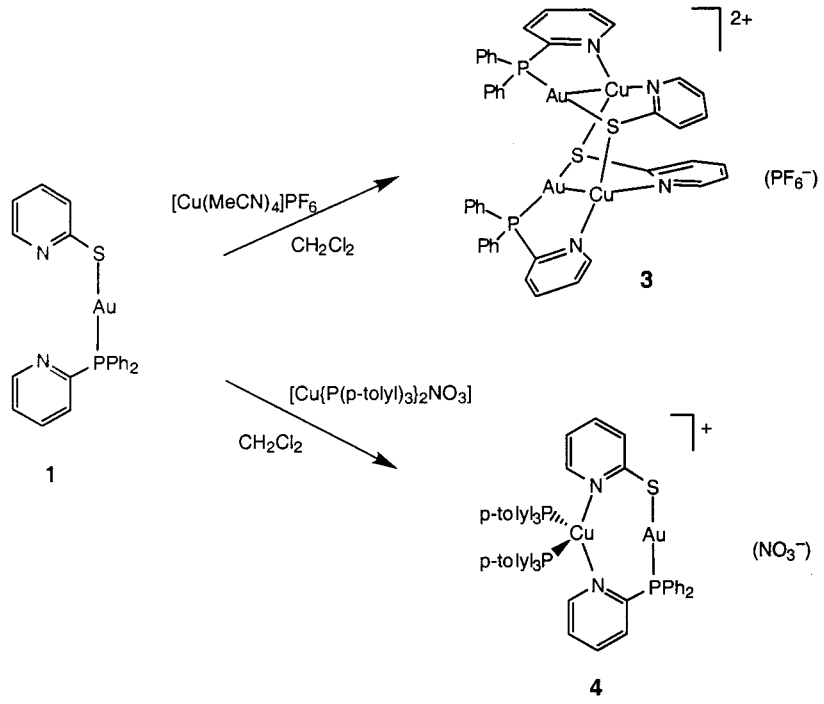

dimerization of AuCu(μ-Spy)(μ-PPh_2py) in which the Spy ligand adopts an additional connection to the Cu(I) ions by μ-S ligation. In this manner, a distorted tetrahedral coordination geometry at Cu(I) is attained with bonds to the pyridine N atoms of Spy and PPh_2py ligands, the μ-S of a second Spy ligand, and a Au(I) ion. The Au(1)···Cu(1) and Au(2)···Cu(2) distances are 2.634(1) and 2.646(1) Å, respectively, indicating a strong metal−metal interaction within the "monomer" units of **3**. While Figure 3 suggests C_2 symmetry for the inner core of the complex, deviations from that symmetry are clearly evidenced. For example, the intermonomer Au(1)···Cu(2) distance of 3.108(1) Å indicates a weak degree of metal−metal interaction while the other intermonomer distance for Au(2)···Cu(1) of 3.415 Å corresponds to no significant interaction. The Au(1)···Au(2) separation is 3.425 Å, a distance considered long for a significant aurophilic interaction.[17,20,45,46] The coordination geometry at the Au(I) centers is close to linear with P(1)−Au(1)−S(1) and P(2)−Au(2)−S(2) angles 171.45(5)° and 168.79(5)°, respectively.

Absorption and Emission Spectroscopic Results for Complexes 1−4. The absorption and emission spectra of compounds **1**−**4** and their free ligands are summarized in Table 8. In CH_2Cl_2 solution, the absorption spectrum of mononuclear **1** displays intense bands at 266 and 275 (sh) nm (ϵ = 17040, 14560 M^{-1} cm^{-1}) and a relatively weak band at 318 nm (ϵ = 6330 M^{-1} cm^{-1}), while the H-bonded dimer **2** in CH_2Cl_2 solution shows three bands at 266, 276 (sh), and 350 nm (ϵ = 15210, 13640, and 8470 M^{-1} cm^{-1}). These transitions compare with an absorption band at 261 nm (ϵ = 13270 M^{-1} cm^{-1}) for the free PPh_2py ligand, two absorption bands at 292 and 375 nm (ϵ = 14340 and 5430 M^{-1} cm^{-1}) for HSpy in CH_2Cl_2 solution, and two absorption bands at 282 and 359 nm (ϵ = 16060 and 6390 M^{-1} cm^{-1}) for Na^+Spy^- in MeOH solution. On the basis of the similarity of the absorption bands of compounds **1** and **2** at 266 nm in shape and extinction coefficient relative to the band at 261 nm for free PPh_2py ligand, we assign these absorptions for **1** and **2** as intraligand $\pi-\pi^*$ or $n-\pi^*$ transitions of PPh_2py. While the pairs of bands at 275 and 318 nm for **1** and 276 and 350 nm for **2** appear to correspond to transitions for free Spy^- and HSpy suggesting a ligand-based $\pi-\pi^*$ or $n-\pi^*$ assignment, transitions of similar energy have been attributed by Fackler and co-workers to S → Au(I) charge transfers (LMCT).[48,49] The same assignment may pertain here. The absorption spectrum of **3** gives two bands: one at 244 nm (13740 M^{-1} cm^{-1}) which is assigned to the intraligand $\pi-\pi^*$ or $n-\pi^*$ transitions, and the other at 327 nm (3680 M^{-1} cm^{-1}) which is assigned to the metal-centered transition due to the Au−Cu interaction. The absorption spectrum of **4** in CH_2Cl_2 solution displays two bands at 244 and 300 nm (ϵ = 77550 and 6530 M^{-1} cm^{-1}). The former band is readily assigned to the intraligand $\pi-\pi^*$ or $n-\pi^*$ transition while the latter is attributed to a S → Au(I) charge transfer (LMCT) transition; in complex **4** with a tetrahedrally coordinated Cu(I), a significant Au···Cu interaction appears unlikely (vide infra).

All four complexes exhibit luminescence to varying degrees. For mononuclear complex **1**, emission is weak in the solid state with λ_{max} at 540 nm (380 nm excitation) and extremely weak in fluid solution (λ_{max} of 520 nm). For complexes **2**−**4**, relative emission intensity in both rigid media and fluid solution is increased greatly, although emission in fluid solution appears modest at best. For the H-bonded dimer **2**, the emission maximum in CH_2Cl_2 at ambient temperature is 470 nm with a shoulder near 430 nm (350 nm excitation), while in the solid state, a strong luminescence is seen at 510 nm from excitation at 420 nm. Figure 4 presents both the emission and excitation spectra of **2** in ambient temperature fluid solution. The excitation spectrum shows maxima that coincide with the lowest energy absorption bands. Both **1** and **2** exhibit a blue-shifted emission at ca. 435 nm from 77 K CH_2Cl_2 samples. The tetranuclear Au_2Cu_2 complex **3** luminesces at 610 nm in the solid state, at 635 nm with a 520 nm shoulder in ambient temperature fluid solution, and at 550 nm in a 77 K CH_2Cl_2 frozen sample. The dinuclear AuCu complex **4** shows emission maxima at 510 nm in the solid state, at 510 nm in ambient temperature fluid solution, and at 476 nm with a 440 nm shoulder in frozen CH_2Cl_2 at 77 K. The blue shifts of the emission bands in **1**−**4** in 77

Table 6. Atomic Coordinates ($\times 10^4$) and Equivalent Isotropic Parameters (Å $\times 10^3$) for **3**

	x	*y*	*z*	*U*(eq)[a]		*x*	*y*	*z*	*U*(eq)[a]
Au(1)	2920(1)	1203(1)	4882(1)	31(1)	C(122)	1972(3)	−957(3)	4225(3)	38(1)
Cu(1)	3037(1)	2408(1)	3883(1)	36(1)	C(132)	1342(4)	−1252(4)	4421(4)	45(2)
S(11)	4039(1)	865(1)	4596(1)	37(1)	C(142)	1183(5)	−1390(5)	5185(4)	67(2)
P(11)	1878(1)	1726(1)	5126(1)	28(1)	C(152)	1653(6)	−1213(5)	5758(5)	83(3)
N(11)	2392(2)	3101(3)	4492(3)	32(1)	C(162)	2287(6)	−917(5)	5579(5)	81(3)
N(21)	4045(2)	2440(3)	4083(3)	37(1)	C(172)	2450(4)	−794(4)	4817(4)	58(2)
C(11)	2408(3)	3902(4)	4328(4)	43(1)	C(182)	3388(3)	1844(3)	2228(3)	33(1)
C(21)	1976(4)	4456(4)	4656(4)	48(2)	C(192)	3549(4)	2336(4)	1605(4)	51(2)
C(31)	1527(4)	4192(4)	5202(4)	52(2)	C(202)	4150(4)	2202(5)	1230(4)	62(2)
C(41)	1516(3)	3371(4)	5395(4)	44(2)	C(212)	4572(4)	1596(5)	1487(4)	59(2)
C(51)	1938(3)	2840(3)	5021(3)	30(1)	C(222)	4389(3)	1135(4)	2113(4)	43(1)
C(61)	1220(3)	1444(3)	4415(3)	29(1)	P(1)	479(1)	6250(1)	4035(1)	43(1)
C(71)	1097(3)	1895(4)	3737(3)	35(1)	F(1)	−237(4)	5957(6)	3625(5)	49(2)
C(81)	648(3)	1622(4)	3181(4)	41(1)	F(1A)	−225(7)	6275(8)	3548(8)	91(4)
C(91)	294(3)	888(4)	3281(4)	43(1)	F(2)	1185(6)	6564(8)	4350(7)	93(4)
C(101)	403(3)	451(4)	3947(4)	43(1)	F(2A)	1117(5)	6187(7)	4621(6)	74(3)
C(111)	874(3)	712(4)	4520(3)	36(1)	F(3)	928(6)	6155(7)	3259(7)	71(3)
C(121)	1524(3)	1479(3)	6056(3)	30(1)	F(3A)	830(6)	5849(8)	3309(7)	76(4)
C(131)	847(3)	1650(4)	6221(3)	35(1)	F(4)	360(5)	7096(6)	3571(6)	62(2)
C(141)	587(3)	1401(4)	6919(4)	42(1)	F(4A)	544(7)	7182(8)	3959(8)	101(4)
C(151)	989(3)	969(4)	7443(4)	46(2)	F(5)	56(5)	6322(6)	4783(5)	61(2)
C(161)	1647(4)	803(4)	7286(4)	48(2)	F(5A)	74(5)	6711(6)	4736(5)	61(2)
C(171)	1926(3)	1050(4)	6584(3)	38(1)	F(6)	516(7)	5279(8)	4112(8)	97(4)
C(181)	4422(3)	1813(4)	4355(3)	37(1)	F(6A)	442(9)	5445(11)	4500(10)	129(6)
C(191)	5129(3)	1865(5)	4453(4)	51(2)	P(2)	6149(1)	−60(1)	2769(1)	60(1)
C(201)	5441(4)	2592(6)	4277(5)	71(2)	F(7)	5506(4)	248(5)	3315(4)	49(2)
C(211)	5058(4)	3231(5)	4003(5)	66(2)	F(7A)	5769(8)	633(9)	3164(8)	115(4)
C(221)	4377(4)	3134(4)	3909(4)	50(2)	F(8)	6688(6)	−397(8)	2204(7)	82(4)
Au(2)	2306(1)	713(1)	3062(1)	30(1)	F(8A)	6649(6)	−706(7)	2344(7)	72(3)
Cu(2)	3618(1)	542(1)	3410(1)	37(1)	F(9)	6577(5)	−99(7)	3584(6)	67(3)
S(12)	2611(1)	2032(1)	2704(1)	33(1)	F(9A)	6482(7)	−432(9)	3484(8)	92(4)
P(12)	2165(1)	−645(1)	3244(1)	31(1)	F(10)	5817(6)	−966(7)	3015(7)	90(3)
N(12)	3541(3)	−684(3)	3241(3)	39(1)	F(10A)	5579(8)	−594(10)	2582(10)	132(5)
N(22)	3808(2)	1250(3)	2488(3)	33(1)	F(11)	6300(8)	803(9)	2655(8)	116(4)
C(12)	4159(3)	−1031(4)	3159(5)	53(2)	F(11A)	6790(7)	597(8)	2697(8)	106(4)
C(22)	4249(4)	−1796(5)	2864(5)	63(2)	F(12)	5924(8)	407(9)	1954(8)	119(4)
C(32)	3688(4)	−2242(5)	2631(5)	66(2)	F(12A)	5624(5)	−117(7)	2049(6)	74(3)
C(42)	3046(4)	−1905(4)	2727(4)	51(2)	C(1S)	3473(4)	−688(5)	2(5)	60(2)
C(52)	2990(3)	−1129(3)	3049(4)	37(1)	C(2S)	3075(4)	−795(5)	631(4)	56(2)
C(62)	1544(3)	−1111(3)	2592(3)	32(1)	C(3S)	2590(4)	−1394(5)	636(5)	62(2)
C(72)	1225(3)	−620(4)	2026(3)	39(1)	C(4S)	2503(5)	−1910(6)	67(7)	84(3)
C(82)	779(3)	−958(4)	1487(4)	44(2)	C(5S)	2889(7)	−1841(8)	−569(8)	116(4)
C(92)	637(3)	−1785(4)	1516(4)	45(2)	C(6S)	3389(6)	−1223(8)	−629(6)	99(4)
C(102)	929(3)	−2264(4)	2088(4)	40(1)	Cl(1)	4083(1)	55(2)	−36(2)	100(1)
C(112)	1378(3)	−1933(3)	2632(3)	34(1)	Cl(2)	3133(2)	−102(2)	1378(1)	109(1)

[a] *U*(eq) is defined as one-third of the trace of the orthogonalized $\mathbf{U}_{ij}$ tensor.

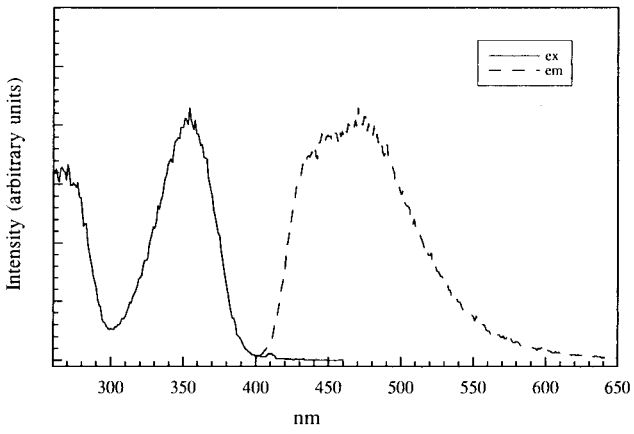

Figure 4. Emission and excitation spectra of **2** (2×10^{-5} M) in ambient temperature CH_2Cl_2 solution.

K frozen media relative to ambient temperature fluid solutions have been observed with other luminescent complexes and are due to "luminescence rigidochromism", i.e., the dependence of emission energy on environmental rigidity.[32,54,55] The free ligands 2-SpyH, PPh_2py, and NaSpy also show very weak emission in both solution and the solid state in the region of 430−470 nm.

On the basis of the data summarized above, the assignment of the emissive state in complexes **1**−**4** is uncertain. Key guidance can be found in the study by Fackler and co-workers on Au(I) tertiary phosphine arylthiolate complexes in which the phosphines employed were PPh_3 and 1,3,5-triaza-7-phosphaadamantane (TPA), and the arylthiolates had Cl and OMe substituents in different positions.[48] In the study, emission maxima were found over a wide range of values (413−700 nm) and were assigned principally to S(pπ) → Au LMCT transitions. In general, the PPh_3 complexes emitted at higher energies than the TPA derivatives. It was suggested that at least two factors influenced the emission energies in these systems. First, substituents on the arylthiolate ligands alter the S(pπ) HOMO energy, and second, the degree of Au···Au interaction modifies the position of the Au pσ LUMO (σ referring to the Au orbital

(54) Lees, A. J. *Chem. Rev.* **1987**, *87*, 711.
(55) Ferraudi, G. J. In *Elements of Inorganic Photochemistry*; John Wiley & Sons: New York, 1988.

Table 7. Selected Bond Distances (Å) and Angles (deg) for **3**

Au(1)−P(11)	2.2678(13)	P(11)−C(121)	1.809(5)	Cu(2)−N(22)	2.011(5)
Au(1)−S(11)	2.3314(14)	P(11)−C(61)	1.817(6)	Cu(2)−N(12)	2.033(5)
Au(1)−Cu(1)	2.6339(7)	P(11)−C(51)	1.838(6)	S(12)−C(182)	1.778(6)
Au(1)−Cu(2)	3.1084(8)	N(11)−C(11)	1.343(7)	P(12)−C(62)	1.805(6)
Cu(1)−N(21)	2.000(5)	N(11)−C(51)	1.360(7)	P(12)−C(122)	1.816(6)
Cu(1)−N(11)	2.016(5)	N(21)−C(181)	1.345(8)	P(12)−C(52)	1.842(6)
Cu(1)−S(12)	2.263(2)	N(21)−C(221)	1.347(8)	N(12)−C(52)	1.340(8)
S(11)−C(181)	1.779(6)	Au(2)−P(12)	2.2655(14)	N(12)−C(12)	1.351(8)
S(11)−Cu(2)	2.247(2)	Au(2)−S(12)	2.3287(14)	N(22)−C(222)	1.340(7)
		Au(2)−Cu(2)	2.6455(7)	N(22)−C(182)	1.344(7)
P(11)−Au(1)−S(11)	171.45(5)	C(121)−P(11)−Au(1)	116.7(2)	N(12)−Cu(2)−Au(1)	115.4(2)
P(11)−Au(1)−Cu(1)	86.12(4)	C(61)−P(11)−Au(1)	114.1(2)	S(11)−Cu(2)−Au(1)	48.39(4)
S(11)−Au(1)−Cu(1)	86.60(4)	C(51)−P(11)−Au(1)	107.2(2)	Au(2)−Cu(2)−Au(1)	72.56(2)
P(11)−Au(1)−Cu(2)	134.58(4)	C(11)−N(11)−C(51)	117.8(5)	C(182)−S(12)−Cu(1)	99.1(2)
S(11)−Au(1)−Cu(2)	46.12(4)	C(11)−N(11)−Cu(1)	115.0(4)	C(182)−S(12)−Au(2)	101.0(2)
Cu(1)−Au(1)−Cu(2)	71.33(2)	C(51)−N(11)−Cu(1)	127.2(4)	Cu(1)−S(12)−Au(2)	96.10(6)
N(21)−Cu(1)−N(11)	121.9(2)	C(181)−N(21)−C(221)	117.2(5)	C(62)−P(12)−C(122)	107.9(3)
N(21)−Cu(1)−S(12)	120.21(14)	C(181)−N(21)−Cu(1)	125.0(4)	C(62)−P(12)−C(52)	106.8(3)
N(11)−Cu(1)−S(12)	113.43(14)	C(221)−N(21)−Cu(1)	117.8(5)	C(122)−P(12)−C(52)	104.7(3)
N(21)−Cu(1)−Au(1)	90.59(14)	P(12)−Au(2)−S(12)	168.79(5)	C(62)−P(12)−Au(2)	114.4(2)
N(11)−Cu(1)−Au(1)	90.83(13)	P(12)−Au(2)−Cu(2)	89.22(4)	C(122)−P(12)−Au(2)	115.7(2)
S(12)−Cu(1)−Au(1)	110.24(4)	S(12)−Au(2)−Cu(2)	84.45(4)	C(52)−P(12)−Au(2)	106.6(2)
C(181)−S(11)−Cu(2)	98.1(2)	N(22)−Cu(2)−N(12)	118.1(2)	C(52)−N(12)−C(12)	117.9(5)
C(181)−S(11)−Au(1)	104.4(2)	N(22)−Cu(2)−S(11)	120.77(14)	C(52)−N(12)−Cu(2)	129.0(4)
Cu(2)−S(11)−Au(1)	85.49(5)	N(12)−Cu(2)−S(11)	112.8(2)	C(12)−N(12)−Cu(2)	111.5(4)
C(121)−P(11)−C(61)	104.9(2)	N(22)−Cu(2)−Au(2)	87.62(14)	C(222)−N(22)−C(182)	117.7(5)
C(121)−P(11)−C(51)	109.7(2)	N(12)−Cu(2)−Au(2)	90.22(14)	C(222)−N(22)−Cu(2)	118.5(4)
C(61)−P(11)−C(51)	103.5(2)	S(11)−Cu(2)−Au(2)	120.95(5)	C(182)−N(22)−Cu(2)	123.8(4)
		N(22)−Cu(2)−Au(1)	122.59(13)		

Table 8. Absorption and Emission Data of Compounds **1**−**4** and Related Ligands

	UV−vis[a]	emission λ_{max}, nm		
complex	λ_{max}, nm (ϵ, M^{-1} cm^{-1})	solid[b], 77 K	fluid soln[a], 298 K	frozen soln[a], 77 K
Au(Spy)(PPh_2py) (**1**)	266 (17040) 275 (14560) 318 (6330)	544	520 437	432
[{Au(SpyH)(PPh_2py)}$_2$](PF_6)$_2$ (**2**)	266 (15210) 276 (13640) 350 (8470)	510	470 432	438
[{AuCu(μ-Spy)(μ-PPh_2py)}$_2$](PF_6)$_2$ (**3**)	254 (13740) 327 (3680)	610	635 520	554
[AuCu(P(*p*-tolyl)$_3$)$_2$(μ-Spy)(μ-PPh_2py)](NO_3) (**4**)	244 (77550) 300 (6530)	508	510 435	476
2-SpyH[c]	292 (14340) 375 (5430)	469	432	479
PPh_2py[c]	261 (13270)	434 467 (sh)	436	478
Na^+Spy^-	282 (16060) 359 (6390)	460	553	490

[a] In CH_2Cl_2 solution, 2×10^{-5} M. [b] Measured in quartz tube with inner diameter of 3 mm, sample height: 1.5 cm. [c] In CH_2Cl_2 solution, 4×10^{-5} M. [d] In MeOH solution, 4×10^{-4} M.

oriented along the Au···Au direction). The authors conclude that emission maxima cannot be used to predict the presence of aurophilic interactions but that the latter can shift the LMCT emission maxima to lower energies.[48]

It is evident that additional work is necessary, including the preparation of systematically modified derivatives, in order to make definitive assignments of the emitting states of **1**−**4**, but certain conclusions can be drawn at this point. First, emission intensity is significantly greater in compounds **2**−**4** in which Au···Au or Au···Cu interactions are present. Second, involvement of the pyridylthiolate ligand in H bonding or Cu(I) coordination can be expected to stabilize the S pπ orbital shifting a LMCT transition to higher energy. This is seen for **2** and **4** relative to **1**. Third, the significant degree of Au···Cu interaction in **3** leads to a significant red shift of the LMCT state. Such an interaction is not expected for **4** in which the Cu(I) ion is tetrahedrally coordinated and not thought to have a significant Au···Cu interaction. Fourth, the relatively high energy emissions at ca. 435 nm seen for **1** and **2** in frozen dichloromethane solutions at 77 K may result from pure ligand excited states as the free ligands are found to have very weak emissions at this energy.

Conclusions

The readily accessible compound Au(Spy)(PPh_2py) (**1**) is a useful precursor for the synthesis of heterobimetallic gold complexes and for the linking of Au(I) monomers by supramolecular interactions. The structures of compounds **1**−**3** have been established by single-crystal X-ray structure determination and give us the opportunity to correlate them with their spectroscopic properties. The protonation of monomer **1** results in its dimerization through H bonding to form **2** which exhibits relatively

strong aurophilic interaction. The magnitude of emission intensity is thus greatly increased through the exigency of a "remote" noncovalent interaction. To our knowledge, the tetranuclear Au_2Cu_2 compound **3** is the first example of a luminescent heterobimetallic $d^{10}-d^{10}$ compound with a strong interaction between the two different d^{10} metals. The emission of **1**−**4** is assigned to a S → Au(I) charge transfer (LMCT) transition which is consistent with spectroscopic data and previous studies on related gold(I) phosphine thiolate complexes.[48,49] Our results suggest that while an observed low-energy emission such as in **3** might result from a strong metal−metal interaction in the molecule, a strong metal−metal interaction as in **2** does not necessarily produce a low-energy emission.

Acknowledgment. We wish to thank the National Science Foundation through its grant to the Science and Technology Center for Photoinduced Charge Transfer (CHE-9120001) for support of this research.

Supporting Information Available: X-ray crystallographic files in CIF format for complexes **2** and **5**. This material is available free of charge via the Internet at http://pubs.acs.org.

IC000396F